

# Hydrogen production from biomass woodchips using Ni/CaO–ZrO<sub>2</sub> catalysts

Robert Ryczkowski<sup>1</sup> · Agnieszka M. Ruppert<sup>1</sup> ·  
Piotr Przybysz<sup>2</sup> · Karolina Chałupka<sup>1</sup> ·  
Jacek Grams<sup>1</sup>

Received: 8 December 2016 / Accepted: 15 January 2017 / Published online: 24 January 2017  
© The Author(s) 2017. This article is published with open access at Springerlink.com

**Abstract** This work aimed at the determination of the influence of various types of lignocellulosic biomass on the performance of Ni/ZrO<sub>2</sub> catalyst modified by CaO in the production of hydrogen rich gas from lignocellulosic feedstock. The catalysts were prepared by co-impregnation and sequential impregnation methods. The catalytic activity of the synthesized materials was examined in the high temperature conversion of cellulose (model compound) and real biomass samples—woodchips from pine, beech, birch and poplar. The surface properties of Ni/CaO–ZrO<sub>2</sub> catalysts were characterized by X-ray diffraction (XRD), time-of-flight secondary ion mass spectrometry (ToF–SIMS), thermogravimetric analysis (TG–DTA–MS) and BET methods. The obtained results revealed that an incorporation of calcium into the structure of the catalyst led to a decrease in the coke formation rate on its surface. Moreover, the influence of the preparation method on the material composition and related properties was demonstrated.

**Keywords** Nickel catalyst · Calcium oxide · Zirconium oxide · Biomass conversion · Pyrolysis

## Introduction

Lignocellulosic biomass is a renewable feedstock widely available around the world. However, many difficulties related with its transformation to energy and chemicals are identified, such as high moisture content, unfavorable directions of decomposition, many competing reactions yielding oxygenates instead of

---

✉ Jacek Grams  
jacek.grams@p.lodz.pl

<sup>1</sup> Institute of General and Ecological Chemistry, Lodz University of Technology, Żeromskiego 116, 90-924 Łódź, Poland

<sup>2</sup> Institute of Papermaking and Printing, Lodz University of Technology, Wólczańska 223, 90-924 Łódź, Poland

hydrocarbons etc. The use of heterogeneous catalyst can be one of the solutions for the increase in the efficiency of high temperature treatment of biomass [1–3].

Nickel based catalysts are widely recognized as viable alternatives to noble metals in biomass conversion processes towards valuable products such as hydrogen rich gas [4–6]. The literature data shows that they can also exhibit high activity in steam reforming [7],  $\text{CH}_4\text{--CO}_2$  reforming [8] and methanation [9]. Our earlier investigations revealed [10] that the  $\text{Ni/ZrO}_2$  catalyst is particularly active and selective in the production of hydrogen rich gas from cellulose. One of the main problems associated with the nickel catalyst is its deactivation via carbon deposition [11]. In order to minimize this effect, various dopants can be introduced into the catalyst structure. It was demonstrated that calcium oxide acts as the substance which is able to hinder the growth of carbonaceous deposit due to gasification of formed coke and enhance in situ regeneration of an active phase, which in turn increases the catalyst activity [12]. It was showed that calcium can incorporate into the lattice of zirconia creating mobile oxygen species that can further enhance efficiency of catalysts and change the mechanism of biomass conversion process [13].

Previous studies demonstrated that  $\text{Ni/CaO--ZrO}_2$  catalysts can be successfully applied in several chemical processes. Si et al. [14] used this system in methane trireforming, a process that allows the formation of  $\text{H}_2$  and  $\text{CO}$  during the reaction with water, oxygen or carbon dioxide, the use of catalysts allowed to exceed 70% methane conversion. Nie et al. [15] applied calcium as a catalyst in lignocellulosic biomass pyrolysis to bio-oil and confirmed that this metal has an impact on the oxygen content and stability of the produced bio-oil directly changing the mechanism of biomass decomposition process leading to the formation of ketones and esters and subsequent reduction of the amount of aromatics.

Our earlier investigation confirmed the positive effect of the addition of calcium on the enhancement of hydrogen yield in the high temperature conversion of cellulose carried out in the presence of  $\text{Ni/ZrO}_2$  catalyst [16]. However, the impact of the method of calcium incorporation into the catalyst structure has not been yet studied, so we decided to determine the influence of Ca introduction method to the  $\text{Ni/ZrO}_2$  system on its catalytic and physicochemical properties. Moreover, the literature data demonstrated that the activity of Ni based systems dropped considerably in the presence of real biomass samples due to more complex composition of the used feedstock (i.e. presence of lignin or different organic and inorganic contaminants) [17]. Therefore, we also focused in this work on the investigation of the influence of various types of biomass on the performance of  $\text{Ni/ZrO}_2$  catalyst modified by  $\text{CaO}$  in the production of hydrogen rich gas.

## Experimental

### Catalyst preparation

$\text{ZrO}_2$  was prepared from  $\text{ZrOCl}_2 \cdot 8\text{H}_2\text{O}$  [Sigma-Aldrich, pure for analysis ( $\geq 99.5\%$ )] by the method described in [16], this material was further used as a support for the catalysts.

For the samples modified with calcium oxide, two different approaches were used. First, in the case of the 20%Ni/10%CaO/ZrO<sub>2</sub> COIMP sample, Ca(NO<sub>3</sub>)<sub>2</sub>·6H<sub>2</sub>O (Sigma-Aldrich, 99.9%), and Ni(NO<sub>3</sub>)<sub>2</sub>·6H<sub>2</sub>O [Chemland, pure for analysis (≥99.5%)] were dissolved in 20 ml of water and added to the beaker containing around 10 g of ZrO<sub>2</sub>. The mixture was stirred for several minutes and aged for 24 h at room temperature. Then water was evaporated and after drying at 120 °C for 2 h, the sample was calcined in air flow at 700 °C for 3 h. Second, for the 20%Ni/10%CaO/ZrO<sub>2</sub> 2xIMP sample, Ca(NO<sub>3</sub>)<sub>2</sub>·6H<sub>2</sub>O (Sigma-Aldrich, 99.9%) was dissolved in 20 ml water and added to the beaker containing ZrO<sub>2</sub>. After aging for 24 h at room temperature, evaporation of water and drying at 120 °C for 2 h, the sample was calcined in air flow at 700 °C for 3 h, put into the beaker again and mixed with Ni(NO<sub>3</sub>)<sub>2</sub>·6H<sub>2</sub>O (Chemland, pure for analysis (≥99.5%)), which was dissolved in water. After that, the obtained material was aged for 24 h. Water was evaporated under the same conditions as for the first sample and finally the catalyst (about 10 g) was calcined second time in air flow at 700 °C for 3 h.

The reference 20%Ni/ZrO<sub>2</sub> catalyst (about 5 g) was synthesized by impregnation of zirconia with Ni(NO<sub>3</sub>)<sub>2</sub>·6H<sub>2</sub>O (Chemland, pure for analysis (≥99.5%)) using the same conditions of treatment as in the previous cases—this sample will be referred as Ni/Zr (Table 1).

### Catalyst characterisation

The surface area and porosity measurements were carried out on an automatic sorptometer Micromeritics ASAP 2020 V3.05 G using N<sub>2</sub> as adsorbent at −196 °C, with a prior outgassing at 200 °C for 3 h in order to desorb the impurities or moisture. The Brunauer–Emmett–Teller (BET) specific surface area was calculated from the N<sub>2</sub> adsorption isotherm.

Powder X-ray diffractograms (XRD) were collected using a PANalytical X'Pert Pro MPD diffractometer. The X-ray source was a copper long fine focus X-ray diffraction tube operating at 40 kV and 30 mA. Data were collected in the 10°–90° 2θ range with 0.0167° step. Crystalline phases were identified by references to ICDD PDF-2 (version 2004) database. All calculations were performed with X'Pert High Score Plus computer program. Crystalline size was calculated with the Scherrer method.

Time-of-flight secondary ion mass spectrometry (ToF–SIMS) was applied to the characterization of the surface composition of prepared catalysts. The measurements were performed using the ION-TOF GmbH instrument (ToF–SIMS IV) equipped with 25 kV pulsed Bi<sup>+</sup> primary ion gun in the static mode. The analyzed area corresponded to a square of 500 μm × 500 μm. Before the measurements, the

**Table 1** Abbreviations of the catalysts used in this work

Sample name	Abbreviation
20%Ni/ZrO <sub>2</sub>	Ni/Zr
20%Ni/10%CaO/ZrO <sub>2</sub> COIMP	Ni/Ca/Zr COIMP
20%Ni/10%CaO/ZrO <sub>2</sub> 2xIMP	Ni/Ca/Zr 2xIMP

samples were pressed into pellets and attached to the sample holder using a double-sided tape. Moreover, a pulsed electron flood gun was used for charge compensation.

Thermogravimetric and differential thermal analysis (TGA–DTA–MS) has been performed using the derivatograph SETSYS 16/18, Setaram and mass spectrometer ThermoStar, Balzers. The TGA–DTA and MS spectra were recorded in the air flow ( $40 \text{ ml min}^{-1}$ ) in the temperature range of 15 to  $900^\circ\text{C}$  with a heating rate of  $10^\circ\text{C min}^{-1}$ . The sample mass was varied between 5 and 20 mg and the samples were weighed in the corundum crucible. These studies were performed in order to determine the amount of carbon deposited on the catalyst during the cellulose decomposition process.

### Catalyst activity

The activity of the investigated catalysts was tested in quartz fixed bed two step reactor. Biomass decomposition ( $500^\circ\text{C}$ ) was separated from the catalyst bed ( $700^\circ\text{C}$ ), where subsequent products upgrading occurred. The products were transported through the reactors to gas capture syringe by the flow of argon ( $15 \text{ cm}^3 \text{ min}^{-1}$ ). Then the chromatographic analysis took place with GC-TCD (Agilent 7820A) using packed column Agilent 6Ft 1/8 2 mm Molsieve 5A 60/80 SS. The amounts of  $\text{H}_2$ , CO,  $\text{CO}_2$  and  $\text{CH}_4$  were determined. The separation of hydrogen and carbon dioxide was achieved in  $80^\circ\text{C}$ , then the temperature was increased to  $120^\circ\text{C}$  to evaluate the amount of methane and carbon monoxide. A larger part of heavier molecules was removed from the gaseous mixture by their condensation before GC measurements. However, the presence of a small amount of i.e. light hydrocarbons could not be excluded. The amount of  $\text{H}_2$ , CO,  $\text{CO}_2$  and  $\text{CH}_4$  was determined via EzChrom Elite software. In each case, 0.4 g of biomass and 0.1 g of the catalyst were used. The  $\alpha$ -cellulose (Sigma-Aldrich, pure)—reference material and real biomass samples were applied as a feedstock.

### Biomass woodchips

Different types of biomass, beech, birch, poplar and pines pulps, submitted to the delignification process, were applied as the feedstock. The solids were disintegrated for 3 min in a laboratory propeller pulp disintegrator (type R1 from Labor-meks). The disintegrated materials in the form of woodchips were kept in hermetically closed vials to avoid any changes in the humidity before the treatment with NaOH and  $\text{Na}_2\text{S}$  solutions, which were prepared freshly before the usage. Delignification processes were conducted in  $15 \text{ dm}^3$  stainless steel reactors. The batch of oven dry woodchips per cycle was 1000 g. Suspensions of woodchips were heated for 120 min to achieve the temperature of  $160^\circ\text{C}$  for poplar,  $165^\circ\text{C}$  for birch and beech and  $172^\circ\text{C}$  for pine and incubated at this temperature for the next 120 min. Then the temperature was decreased to the ambient one using cold tap water and the insoluble residue was separated by filtration on Buchner funnel, washed several times with demineralized water and incubated overnight in demineralized water to remove residues of the alkali-soluble fractions. The obtained pulps were processed

using a membrane screener equipped with 0.2 mm gaps screening plate. Triplicate samples of fibers after screening were analyzed for the residual lignin contents. The amount of main constituents of the biomass samples is presented in Table 2.

## Results and discussion

### Physicochemical properties

The analysis of BET results (Table 3) demonstrated that unmodified nickel catalyst supported on zirconia possessed highest surface area ( $127 \text{ m}^2 \text{ g}^{-1}$ ). An introduction of calcium to its structure resulted in significant drop in surface area irrespective of the method of Ca incorporation (32 and  $37 \text{ m}^2 \text{ g}^{-1}$  in the case of Ni/Ca/Zr COIMP and Ni/Ca/Zr 2xIMP). However, it was also observed that Ca introduction was connected with the increase in the pore size of the studied catalysts from 2.7 nm for Ni/Zr sample to 5.2 and 6.3 in the case of Ni/Ca/Zr COIMP and Ni/Ca/Zr 2xIMP, respectively. This phenomenon was also accompanied by a decrease in the pore volume of the modified materials in comparison to unmodified ones.

The XRD diffractograms of studied samples revealed the presence of diffraction lines at  $2\theta$  values of  $37.2^\circ$ ,  $43.1^\circ$ ,  $62.8^\circ$ ,  $75.3^\circ$ ,  $79.4^\circ$ , and  $29.8^\circ$ ,  $34.8^\circ$ ,  $49.5^\circ$ ,  $59.4^\circ$  originating from NiO and  $\text{ZrO}_2$  tetragonal phase, respectively (Fig. 1). The

**Table 2** Composition of biomass samples

Name	Cellulose (%)	Hemicelluloses (%)	Lignin (%)
Cellulose (Sigma-Aldrich)	100	–	–
Pine A <sup>a</sup>	94.34	2.54	2.58
Pine B <sup>b</sup>	71.65	9.11	12.93
Beech <sup>b</sup>	91.28	4.85	3.87
Birch <sup>b</sup>	92.34	3.42	4.25
Poplar <sup>c</sup>	95.63	2.06	2.31

<sup>a</sup> Sample treated with 266 g NaOH and 114 g  $\text{Na}_2\text{S}$  per kg wood during delignification

<sup>b</sup> Sample treated with 140 g NaOH and 60 g  $\text{Na}_2\text{S}$  per kg wood during delignification

<sup>c</sup> Sample treated with 182 g NaOH and 78 g  $\text{Na}_2\text{S}$  per kg wood during delignification

**Table 3** Physicochemical properties of the investigated catalysts

	Surface area ( $\text{m}^2 \text{ g}^{-1}$ )	Pore size (nm)	Pore volume ( $\text{cm}^3 \text{ g}^{-1}$ )	NiO crystallite size (nm) (XRD)
Ni/Ca/Zr COIMP	32	5.2	0.11	18
Ni/Ca/Zr 2xIMP	37	6.3	0.12	28
Ni/Zr	127	2.7	0.21	26

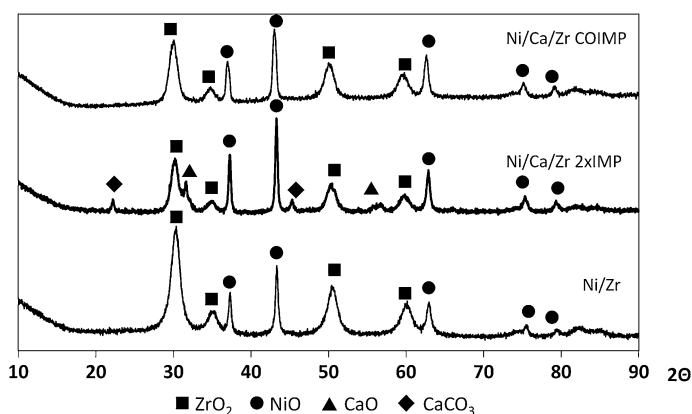


**Fig. 1** X-ray diffraction patterns of the investigated catalysts

diffraction lines corresponding to the presence of calcium species in the form of CaO and  $\text{CaCO}_3$  was observed only for Ni/Ca/Zr 2xIMP sample. The formation of  $\text{CaCO}_3$  may be connected with the conversion of calcium oxide during catalyst treatment in the presence of  $\text{CO}_2$  originating from the atmosphere. Probably, in this case, CaO and  $\text{CaCO}_3$  phases formed well defined and larger crystallites than those noted for Ni/Ca/Zr COIMP sample. CaO might also occur in amorphous phase (especially in the case of the catalyst prepared by the co-impregnation method) making it undetectable during the XRD analysis.

The NiO crystallite size was calculated from the XRD data using the Scherrer method (Table 3). While the size of nickel oxide crystallites deposited on the surface of Ni/Ca/Zr 2xIMP was similar to that observed for the unmodified Ni/ZrO<sub>2</sub> catalyst (26 and 28 nm, respectively), they were smaller (18 nm) for the Ni/Ca/Zr COIMP sample.

ToF–SIMS spectra collected from the surface of the Ni/Ca/Zr COIMP sample showed the presence of a larger amount of Ca in relation to Ni and Zr than in the case of the catalyst prepared by the sequential impregnation method ( $\text{Ca}^+/\text{Ni}^+$ —1.9 and 1.2; and  $\text{Ca}^+/\text{Zr}^+$ —33 and 18, see Table 4). In spite of that, almost the same content of surface accessible Ni deposited on zirconia was observed in both cases. However, the value of  $\text{Ni}^+/\text{Zr}^+$  ion ratio was higher for unmodified Ni/Zr catalyst. It suggested the presence of a larger amount of Ni species on the surface of that sample.

**Table 4** Relative intensities of selected ions calculated on the basis of ToF–SIMS spectra collected from the surface of investigated catalysts

	$\text{Ca}^+/\text{Ni}^+$	$\text{Ca}^+/\text{Zr}^+$	$\text{Ni}^+/\text{Zr}^+$
Ni/Zr	—	—	22
Ni/Ca/Zr COIMP	1.9	33	17
Ni/Ca/Zr 2xIMP	1.2	18	16

## Catalyst activity measurements

The activity of modified Ni/CaO–ZrO<sub>2</sub> catalysts was investigated in the high temperature conversion of both cellulose and delignified woodchips samples towards hydrogen rich gas. Furthermore, the measurements without catalyst and with the use of reference Ni/ZrO<sub>2</sub> sample were performed for comparison. The activity tests revealed that besides gaseous fraction also liquid phase and solid residue (carbonaceous material) were formed.

Chromatographic analysis of the obtained gas mixture revealed that the main gaseous products of the studied process were: hydrogen, carbon dioxide, carbon oxide and methane (Table 5).

As compared with the results obtained for the non-catalyzed process, the presence of Ni/ZrO<sub>2</sub> catalyst enhanced both the total volume of the gas mixture that can be obtained from cellulose and H<sub>2</sub> content. A further increase of H<sub>2</sub> yield was observed when calcium was added. However, a slightly higher activity was noted for the sample obtained by the co-impregnation method.

## Investigation of carbon deposition

The main problem related with the use of nickel catalysts for the thermochemical conversion of lignocellulosic biomass is linked with the formation of carbon deposit on its surface and in consequence their deactivation. The TG–DTA–MS analysis was performed in order to evaluate the amount and type of coke that was accumulated during the cellulose decomposition process on the surface of the most active Ni/Ca/Zr COIMP and unmodified Ni/Zr catalysts (Figs. 2 and 3). The obtained results indicated that the content of carbon deposited on the Ca doped sample was about 20% lower in comparison to reference Ni/Zr catalyst (5.37 and 6.64 mg). In the case of the unmodified sample, TG–DTA and MS spectra (signal at  $m/z = 44$  originated from CO<sub>2</sub>) revealed the presence of only one type of carbon deposit (most likely carbon whiskers) decomposing in the temperature range from about 300–600 °C (with the maximum of the CO<sub>2</sub> formation rate between 500 and 600 °C) [18]. For Ni/Ca/Zr COIMP, in addition to the main peak, the signals with the maxima at about 400 °C and slightly above 600 °C were also observed. This may indicate the presence of different carbon forms. However, the signal with the maximum between 500 and 600 °C still remains the major one in the latter case. According to literature data, for nickel catalysts operating in high temperatures,

**Table 5** Production of gaseous products in the process performed with the use of cellulose as a model compound

	Yield (mmol g <sup>-1</sup> )			
	H <sub>2</sub>	CO <sub>2</sub>	CH <sub>4</sub>	CO
Without catalyst	1.3	1.2	0.9	6.2
Ni/Zr	14.5	3.4	1.0	9.1
Ni/Ca/Zr COIMP	15.6	3.8	1.1	9.5
Ni/Ca/Zr 2xIMP	15.0	3.7	1.2	9.7

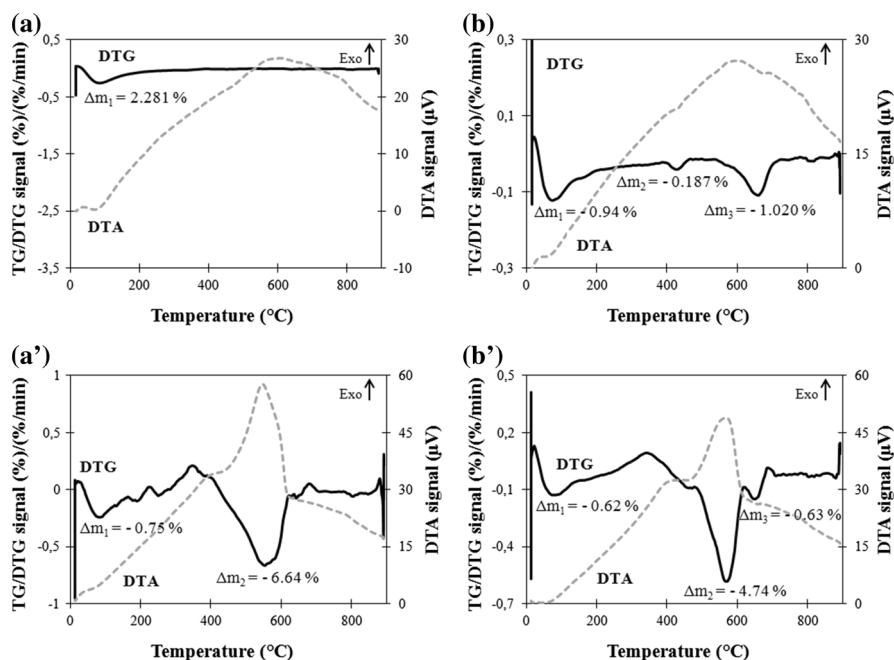


**Fig. 2** DTG–DTA profiles for Ni/Zr as prepared (a) and spent (a') and Ni/Ca/Zr COIMP as prepared (b) and spent (b') catalysts

carbon whiskers are the most common form of deposited coke, which can be accompanied by amorphous or graphitic carbon (peaks at lower and the highest temperature, respectively) [11, 19]. As mentioned earlier, the formation of carbon deposit may be one of the main reasons of catalyst deactivation. An analysis of the changes in the activity of Ni/Ca/Zr COIMP catalyst in five consecutive reaction cycles revealed that the hydrogen production dropped of 19% in comparison to as prepared material.

### Activity in woodchip conversion towards H<sub>2</sub> rich gas

The next step of the studies was devoted to the investigation of the performance of the catalysts in the conversion of real biomass samples. Taking into account the lower susceptibility for coke formation of the Ca doped catalyst, only these samples were selected for further measurements. The performed activity tests revealed that the use of woodchips resulted in a decrease in the amount of the produced hydrogen in comparison to the process carried out with cellulose as a feedstock (Table 6). That drop can be connected with the presence of lignin in woodchips samples, which was not totally removed during delignification. Lignin decomposition is more severe in comparison to cellulose. Additionally, the formation of heavier reaction intermediates to larger extend is facilitated, which can consequently be deposited on the catalyst surface and block its active sites.



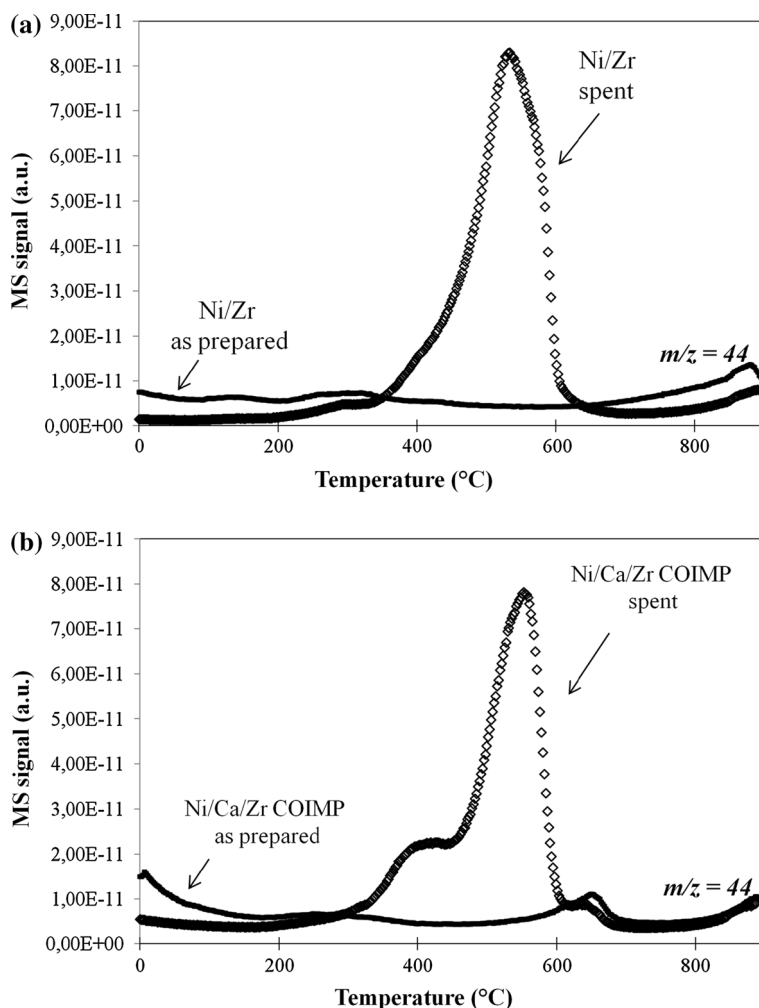


**Fig. 3** MS profiles for  $m/z = 44$  (CO<sub>2</sub>) obtained for **a** as prepared and spent Ni/Zr and **b** Ni/Ca/Zr COIMP catalysts

The hydrogen yield obtained with the use of beech, birch, poplar and pine B was similar in spite of that the last sample consisted of larger amount of lignin (see Table 2). On the other hand, pine A, containing lignin on a similar level as beech, birch, poplar, allowed the production a higher volume of H<sub>2</sub>. Those differences in the H<sub>2</sub> yield may be connected with the various amount of NaOH and Na<sub>2</sub>S used for delignification and still present in the biomass samples. Pine A, allowing for the production of the largest amount of hydrogen, was submitted to delignification carried out with the use of the highest amount of above mentioned chemical reagents. Sodium ions remained in the biomass sample after the treatment can act as catalyst dopants and take part in enhancement of the conversion of lignocellulose towards hydrogen [16, 20].

**Table 6** Composition of gaseous mixture obtained in high temperature treatment of various biomass samples

	Yield (mmol g <sup>-1</sup> )							
	Ni/Ca/Zr COIMP				Ni/Ca/Zr 2xIMP			
	H <sub>2</sub>	CO <sub>2</sub>	CH <sub>4</sub>	CO	H <sub>2</sub>	CO <sub>2</sub>	CH <sub>4</sub>	CO
Cellulose	15.6	3.8	1.1	9.5	15.0	3.7	1.2	9.7
Pine A	13.7	3.5	1.0	8.9	13.1	3.5	1.1	9.0
Pine B	9.7	2.3	1.0	5.8	10.0	2.3	0.7	6.0
Beech	10.1	2.9	0.8	7.2	9.9	2.8	0.9	7.3
Birch	9.8	2.8	0.8	7.2	9.8	2.8	0.8	7.3
Poplar	9.8	2.8	0.8	7.2	9.3	2.8	0.9	7.4

An analysis of the obtained results confirmed that an addition of calcium impacts the performance of the studied catalysts. It can be attributed to the enhancement of oxygen storage capacity, when divalent cation ( $\text{Ca}^{2+}$ ) is present in  $\text{ZrO}_2$  lattice [21]. The presence of mobile oxygen atoms facilitates removal of carbon deposit formed on the surface of the catalyst by its gasification and formation of  $\text{CO}_2$  [22]. According to Sun et al. [23], coke can be also eliminated in the subsequent  $\text{CO}_2$  pulse by the reverse Boudouard reaction. Owing to that, nickel species remain free from carbon longer time and are ready for the next catalytic acts to occur.

The differences in the performance of the studied catalysts can be ascribed to the presence of nickel phase consisted of smaller Ni crystallites in the case of Ni/Ca/Zr COIMP in comparison to Ni/Zr and Ni/Ca/Zr 2xIMP catalysts. Moreover, in the case of the Ni/Ca/Zr COIMP catalyst, closer contact among smaller Ni crystallites, zirconia and calcium can result in a more efficient transport of oxygen towards metallic phase in comparison to the material prepared by subsequent impregnation.

## Conclusions

An introduction of calcium to the nickel catalyst supported on zirconia has direct impact on its activity and stability. First, it led to a drop of susceptibility to coking during high temperature conversion of lignocellulosic biomass.

The activity tests performed with the use of cellulose revealed that the highest hydrogen yield was obtained for Ni/CaO– $\text{ZrO}_2$  sample prepared by co-impregnation method. This method allowed for smaller NiO crystallites to be formed on the catalyst surface. In spite of that, the difference in the amount of the produced hydrogen among Ni/CaO– $\text{ZrO}_2$  and Ni/ $\text{ZrO}_2$  was not significant. TG–DTA–MS experiments demonstrated that the modified catalyst was more resistant to deactivation.

The experiments conducted with the use of woodchips exhibited that the presence of lignin led to a drop in the activity of the studied catalysts. However, it was also shown that an appropriate biomass pretreatment during this process can enhance the hydrogen production.

**Acknowledgements** The authors would like to thank Dr. Waldemar Maniukiewicz for the XRD measurements and Ms. Zuzanna Bereza for her assistance in the synthesis of catalysts.

**Open Access** This article is distributed under the terms of the Creative Commons Attribution 4.0 International License (<http://creativecommons.org/licenses/by/4.0/>), which permits unrestricted use, distribution, and reproduction in any medium, provided you give appropriate credit to the original author(s) and the source, provide a link to the Creative Commons license, and indicate if changes were made.

## References

1. Navarro RM, Pena MA, Fierro JLG (2007) *Chem Rev* 107:3952–3991
2. Chen D, Liu C (2011) *ChemCatChem* 3:490–511
3. Bridgewater AV (2012) *Biomass Bioenergy* 38:68–94
4. Minowa T, Ogi T (1998) *Catal Today* 45:411–416
5. Matras J, Niewiadomski M, Ruppert A, Grams J (2012) *Kinet Catal* 53:565–569
6. Wu C, Wang Z, Huang J, Williams PT (2013) *Fuel* 106:697–706
7. Nichele V, Signoretti M, Pinna F, Menegazzo F, Rossetti I, Cruciani G, Gerrato G, Di Michele A (2014) *Appl Catal B-Environ* 150–151:12–20
8. Wang C, Si L, Li H, Wen X, Sun N, Zhao N, Wei W, Sun Y (2013) *J Fuel Chem Technol* 41:1204–1209
9. Takano H, Shinomiya H, Izumiya K, Kumagai N, Habazaki H, Hashimoto K (2015) *Int J Hydrogen Energy* 40:8347–8355
10. Ruppert AM, Niewiadomski M, Grams J, Kwapiński W (2014) *Appl Catal B-Environ* 145:85–90
11. Góralski J, Grams J, Paryczak T, Rzeźnicka I (2002) *Carbon* 40:2025–2028
12. Liu S, Guan L, Li J, Zhao N, Wei W, Sun Y (2008) *Fuel* 87:2477–2481
13. Takano H, Shinomiya H, Izumiya K, Kumagai N, Habazaki H, Hashimoto K (2015) *Int J Hydrogen Energy* 40:8347–8355
14. Si L, Wang C, Sun N, Wen X, Zhao N, Xiao F, Wei W, Sun Y (2012) *J Fuel Chem Technol* 40:210–215
15. Nie F, He D, Guan J, Zhang K, Meng T, Zhang Q (2017) *Fuel Process Technol* 155:216–224
16. Ryczkowski R, Niewiadomski M, Michalkiewicz B, Skiba E, Ruppert AM, Grams J (2016) *J Therm Anal Calorim* 126:103–110
17. Grams J, Ruppert AM, Rzeźnicka I, Niewiadomski M, Jędrzejczyk M (2014) *Surf Interface Anal* 46:837–841
18. van Doorn J, Verheul RCS, Singoredjo L, Moulijn JA (1986) *Fuel* 65:1383–1387
19. Tang S-B, Qiu F-L, Lu S-J (1995) *Catal Today* 24:253–255
20. Demirbas A (2010) *Energ Source Part A* 32:1342–1354
21. Wang C, Sun N, Zhao N, Wei W, Sun Y, Sun C, Liu H, Snape C (2015) *Fuel* 143:527–535
22. Liu S, Guan L, Li J, Zhao N, Wei W, Sun Y (2008) *Fuel* 87:2477–2481
23. Sun N, Wen X, Wang F, Peng W, Zhao N, Xiao F, Wei W, Sun Y, Kang J (2011) *Appl Surf Sci* 257:9169–9176